



# Hot embossing of microstructure with moving induction heating and gas-assisted pressuring

Ching-Chieh Kao<sup>1</sup> · Kun-Cheng Ke<sup>1</sup> · Wei-Cheng Hung<sup>1</sup> · Sen-Yeu Yang<sup>1</sup>

Received: 12 July 2019 / Accepted: 18 July 2019 / Published online: 6 August 2019  
© Springer-Verlag GmbH Germany, part of Springer Nature 2019

## Abstract

A new apparatus for a moving induction heating and gas-assisted hot embossing apparatus has been developed. A mechanism was designed and implemented to move the platform in and out the wrapped coil, on which the sealed box for substrate/mold was placed. A chamber of 195 mm diameter and 221 mm length was machined. The movable platform, the sealed box with substrate/mold stack, wrapped coil and cooling fan were all implemented in the high pressure chamber. The nine-point thermocouples attached on the mold, thus, a temperature history of the moving induction heating can be obtained and study the influence of the moving path and power on the heating rate and temperature distribution. The micro V-cut structure hot embossing experiment were performed to prove the potential of this moving induction heating and gas-assisted pressuring hot embossing for fast fabrication of microstructure onto polymeric substrates. As a results, replication rates were all above 95% at 200 °C and 5 kgf/cm<sup>2</sup> and the cycle time was less than 4 min and the optic measurement shows the replicated V-cut film can enhance the 36.8% illuminance. The experiment results show the manufacturing potential of this apparatus.

## 1 Introduction

For the replication of microstructures, hot embossing is one of the most popular fabrication methods. It has the advantages of simple process, low cost and high replication. Hot embossing has often used to produce the microstructure on the surface of biomedical and optical components for enhanced functions. However, there are two major problems in traditional hot embossing. First, the embossing pressure provided by platens is not uniform. Second, the heating and cooling process causes long cycle time.

In order to improve the pressure uniformity, the air cushion pressure and gas-assisted pressurization has been used to provide uniform embossing pressure (Gao et al. 2006; Hocheng and Wen 2008). To shorten the cycle time, some researchers used infrared heating system to reduce the cycle time in 5 min (Chen et al. 2014; Seunarine et al. 2006). In other studies, graphene has been used for rapid heating. Heating rates of 5.48 °C/s could be achieved (Xie

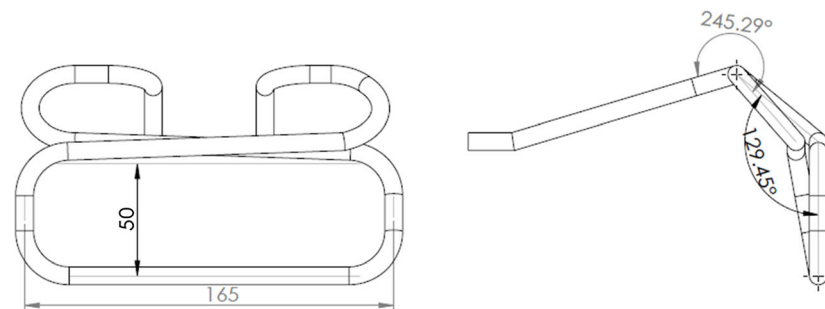
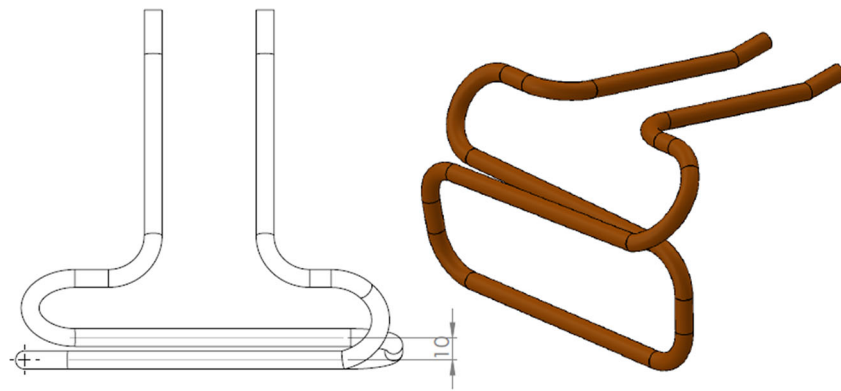
et al. 2014). Induction coil has been used to heat the surface of the mold. Several researchers devoted to improving the uniformity of temperature by coil design (Sun et al. 2013; Nian et al. 2016; Lin et al. 2012). In research of Hong etc., the micro patterns were successfully replicated on a plastic sheet within 60 s by induction heating (Hong et al. 2008). However, the heating area in those studies is limited by the stationary heating system and the heating area restricts the hot embossing area.

In this study, induction heating system and gas-assisted embossing technology in hot embossing process were combined to achieve a high heating rate and uniform pressure. Furthermore, the movable platen mechanism was used to increase the heating area and overcome the embossing area limited by coil length. A set of systematic experiments was conducted to study the influence of the moving path on the heating rate and temperature distribution; then discussed the effect to microstructure replication of pressure and temperature. Besides, the mold used PDMS composite mold instead of metal mold is because the surface microstructure could influence the heating rate and temperature uniformity. According to Yang et al. (2006) research, it showed the direction of microstructure could lead to different heating rates. Furthermore, our study verified the direction of microstructure could seriously

✉ Sen-Yeu Yang  
syyang@ntu.edu.tw

<sup>1</sup> Department of Mechanical Engineering, National Taiwan University, Taipei 106, Taiwan

**Fig. 1** Coil design used in the experiment



Unit: mm

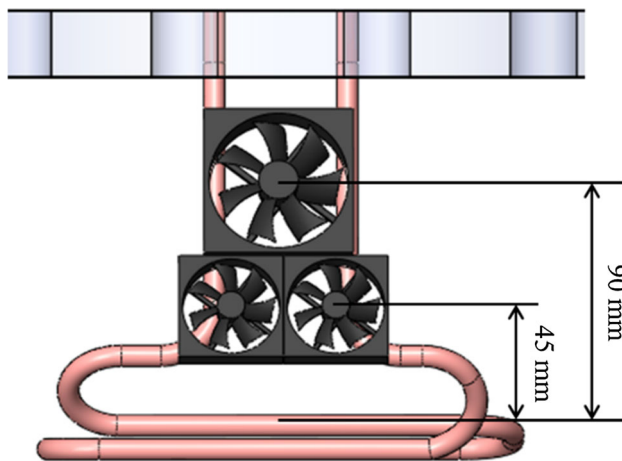


**Fig. 2** Cooling module

affect the heating rate with the different direction of V-cut. Therefore, we proposed a new methodology which PDMS was chosen to be the mold instead of metal mold.

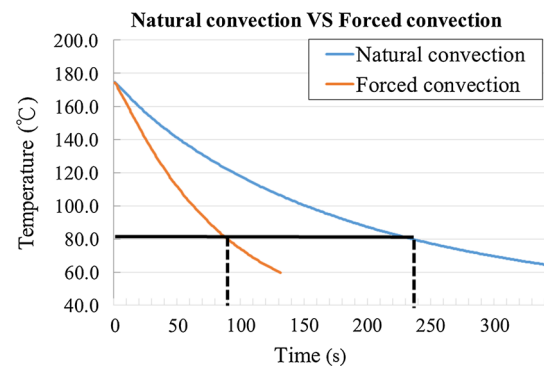


**Fig. 3** Cooling effect

## 2 Principle of induction heating and electromagnetic effect

The high-frequency electromagnetic field is generated around the coil and across the conductor. Because of skin effect, the time-varying magnetic field excited eddy currents inside the conductor and eddy currents  $I_c$  will be concentrated on the surface of the conductor and generated Joule heat.

The skin effect was the phenomenon that the AC current flow in the conductor tends to concentrate the current on

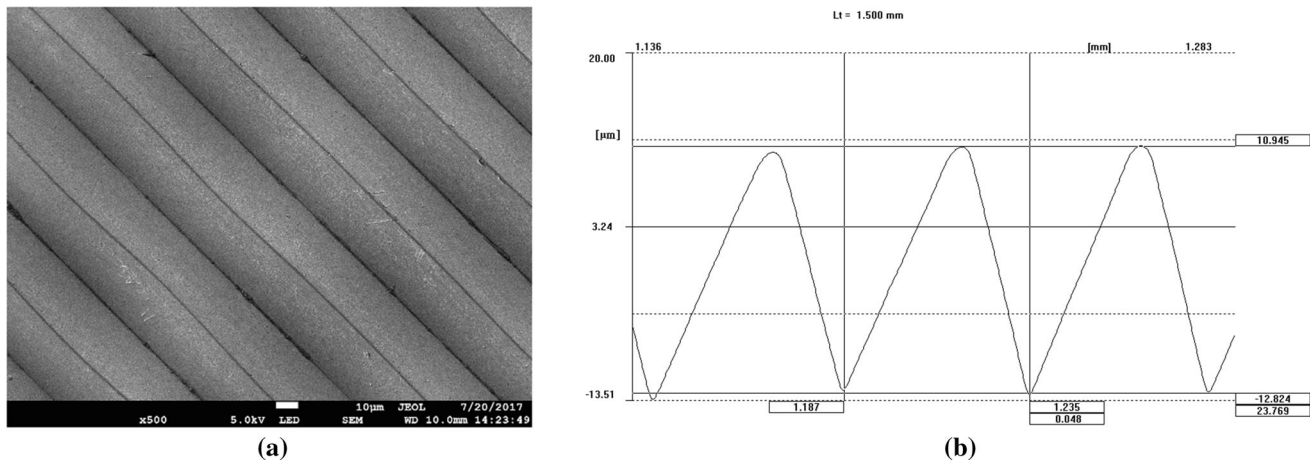
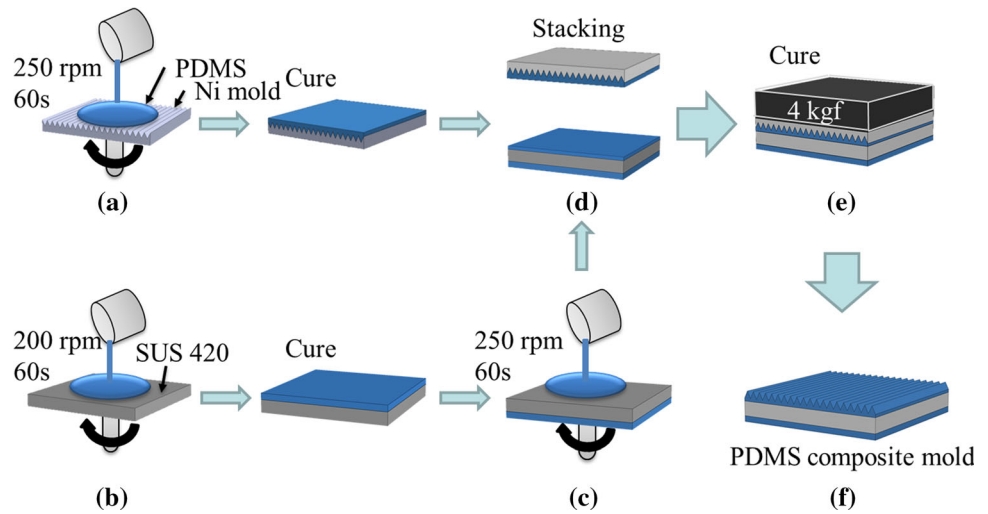


Fig. 4 a SEM image and b surface profiles of the V-cut on the nickel mold

Fig. 5 Schematic showing the fabrication process of PDMS composite mold: a spin coating PDMS on Ni mold and cure, b spin coating PDMS on SUS 420 cure, c spin coating PDMS on the other side of SUS 420, d stack the PDMS which is on the Ni mold, e cured the mold under pressing, f de-molding



the surface and increase the current density which the density distribution was decrease from the surface to inner section. The skin depth  $\delta$  (m) was the depth from the surface to inner section where eddy current density decreased from 100% to 36.8%. It can be expressed by

$$\delta = \sqrt{\frac{\rho}{\pi f \mu}} \tag{1}$$

where  $f$  is the alternating current frequency (Hz),  $\mu$  is the magnetic permeability (H/m) and  $\rho$  is the electrical resistivity ( $\Omega \cdot m$ ). Following by Eq. (1), the conductor with higher magnetic permeability or lower electrical resistivity was much easily to be heated by electromagnetic field under the same alternating current frequency.

### 3 Experiment setup

#### 3.1 Wrapped coil and the cooling fans

In this study, the single turn wrapped coil as shown in Fig. 1. was designed and implemented. The reason for using single-turn wrapped coil, instead of the multi-turn one was that it is easier to control and tailor the temperature raising rate in each area during moving induction process, due to concentrated magnetic field as well as focused heating area.

The cooling module was employed to increase the cooling efficiency and the setup was shown in Fig. 2. The module was setup by one fan of  $6 \times 6 \times 2 \text{ cm}^3$  (H5513B12HD, SEI, Taiwan) and two fans of

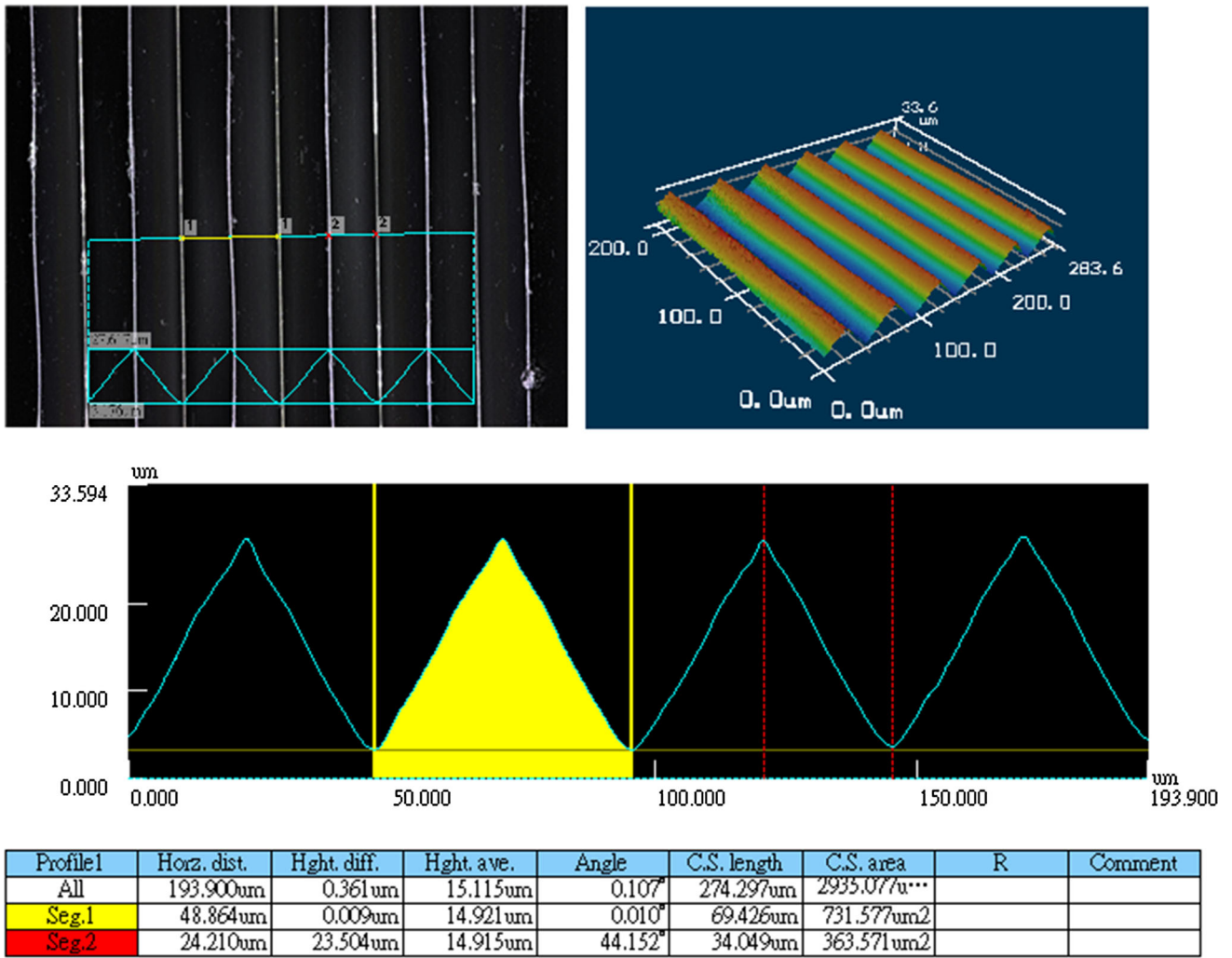
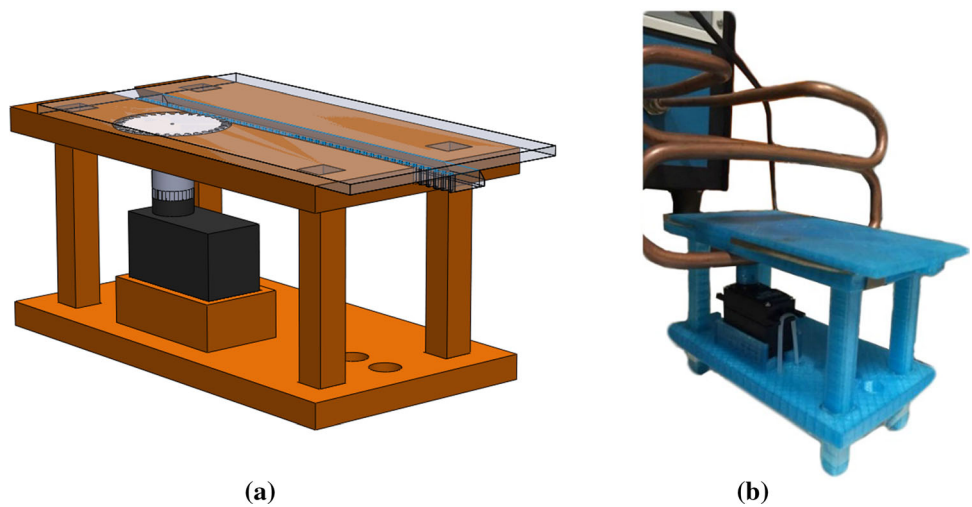


Fig. 6 Confocal image of the V-cut on the PDMS mold

Fig. 7 Movable platform. a 3D sketch and b setup with induction heating coil



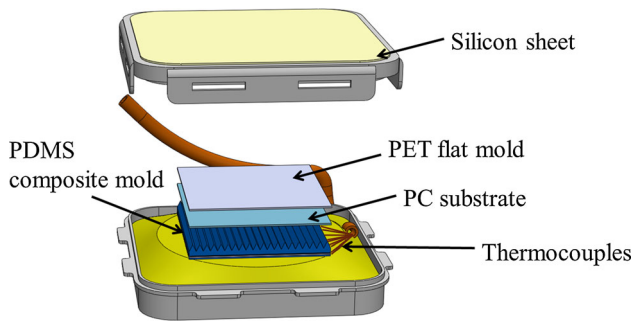


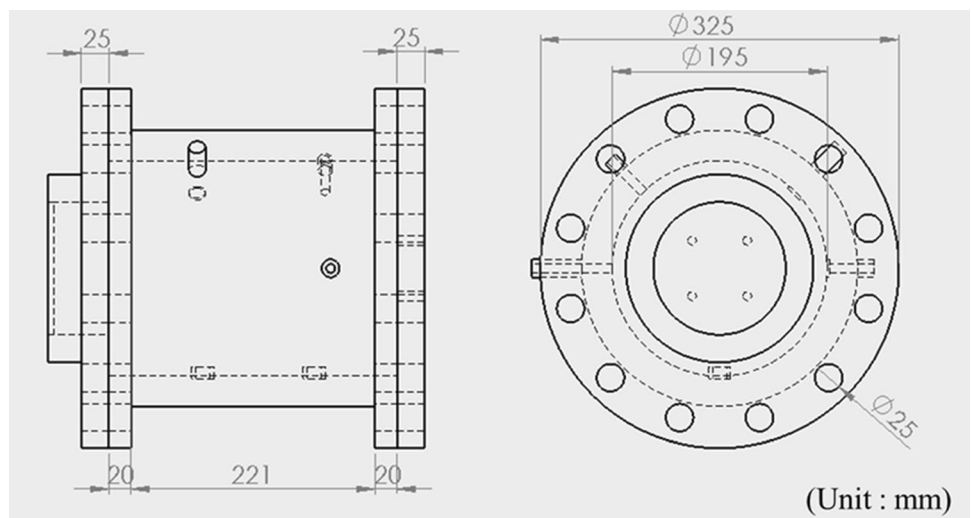
Fig. 8 Sealed box

$4 \times 4 \times 1 \text{ cm}^3$  (U40X12MHZ7-53,NIDEC, China). After comparison, the cooling rate could achieve  $1.25 \text{ }^\circ\text{C/s}$  and greatly reduce more than 50% cooling time than natural cooling, as shown in Fig. 3.

### 3.2 PDMS composite mold and substrate

PDMS is with excellent properties and can be operated over a temperature range from  $-45$  to  $200 \text{ }^\circ\text{C}$ . The advantages of PDMS mold are low cost, excellent replication and easy fabrication. PDMS mold have been used for imprinting and hot embossing (Zhang et al. 2017; Goral et al. 2011). The composite mold was fabricated with 1 mm-thick stainless as insert (SUS 420, Sursun Metals Co., Taiwan) wrapped by PDMS (Sylgard<sup>®</sup> 184, Dow Corning Corporation, USA). This stainless steel platen would be the heat generator for microstructure replication by induction electromagnetic field. The SEM image and surface profile of V-cut microstructure on the Nickel mold is shown in Fig. 4, width and height are  $48 \text{ }\mu\text{m}$  and  $23.76 \text{ }\mu\text{m}$ , respectively. The PDMS composite mold ( $80 \times 80 \text{ mm}^2$ ) manufacturing procedure was shown in Fig. 5.

Fig. 9 Dimension of the chamber



- (a) Spin coating PDMS on the nickel mold 250 rpm for 1 min and cure at  $80 \text{ }^\circ\text{C}$  for 2 h to fabricate a  $0.3 \text{ mm}$  PDMS film.
- (b) Spin coating PDMS on the 420 stainless steel with 200 rpm for 1 min and cure at  $80 \text{ }^\circ\text{C}$  for 2 h to fabricate a  $0.4 \text{ mm}$  PDMS film.
- (c) Spin coating PDMS on the other side of SUS 420 stainless steel with 250 rpm for the 60 s.
- (d) Stacking the nickel mold and SUS 420 with cured and uncured PDMS.
- (e) Cure the mold under 4 kgf pressing at  $80 \text{ }^\circ\text{C}$  for 2 h.
- (f) Peel off the nickel mold at the room temperature and the PDMS composite mold can be obtained..

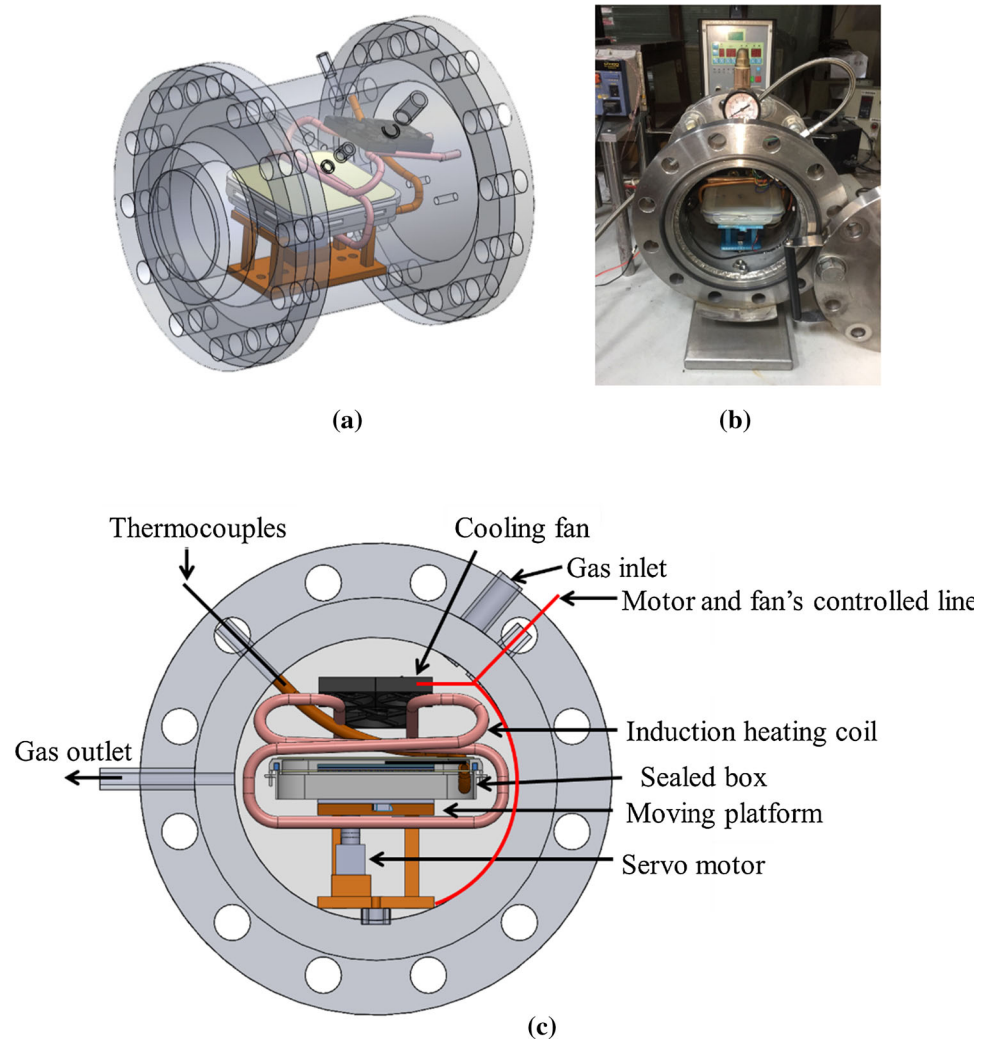
Figure 6 showed the dimension of PDMS structure replicated from the nickel mold with the height of  $23.5 \text{ }\mu\text{m}$  and width of  $48 \text{ }\mu\text{m}$ . The dimension was almost as same as the nickel mold. The PDMS composite mold with microstructure was prepared to replicate the structure on the surface of the PC sheet (Polycarbonate, Lexan8010, GE, USA). The glass transition temperature( $T_g$ ) and dimension of polycarbonate were  $150 \text{ }^\circ\text{C}$  and  $80 \times 80 \times 0.18 \text{ mm}^3$ .

### 3.3 Movable platform and sealed box

Movable platform was driven by GWS S35 servo motor and controlled by Arduino microcontroller board, as shown in Fig. 7b showed the platform setup with the induction heating coil. The platform was made from PLA material by the 3D printer which could avoid to be affected magnetic field during induction heating. In this study, motor speed and the moving path was controlled to achieve a uniform temperature distribution

The top and bottom of sealed box design were made by silicone sheet with a thickness of 1 mm, withstand the

**Fig. 10** **a** Design and **b** photo of the apparatus; **c** section view of the apparatus



temperature to 250 °C and its elastic properties provided uniform pressure by different pressure between the chamber and sealed box, as shown in Fig. 8. The tube inside the sealed box provided the channel for gas and thermocouples went out from the chamber. The thermocouples attached on PDMS surface (without microstructure) were employed to measure the temperature during the hot embossing process. The stack inside the sealed box included PET film, PC film and PDMS composite mold. PET film with a thickness of 0.2 mm is used to keep the PC substrate reaching a smooth surface after hot embossing. PC with a thickness of 0.18 mm is the substrate of hot embossing and the thickness of PDMS composite mold are PDMS with 0.4 mm and SUS420 platen with 1 mm.

### 3.4 High pressure chamber and induction heating module

In Fig. 9, it showed the design of high pressure chamber for this study. The SUS304 stainless steel, which is non-

magnetic to avoid induction heating by electromagnetic field, was employed to be the material of the chamber. The chamber was with two valves, one for gas inlet which provided the pressure for hot embossing and the other one for gas outlet which released the pressure while finishing the hot embossing process. Besides, there were two holes in the chamber connected with sealed box, one for the thermocouple which went through the hole to attach the PDMS composite mold simultaneously and measured the temperature in the hot embossing process; the other hole was for the motor cable. These two holes were sealed with silicon sealant to keep the chamber sealed. The chamber could keep sealed under the under gas pressure 10 kgf/cm<sup>2</sup> which was the highest pressure using in this study.

Figure 10 showed the apparatus for moving induction heating process. The wrapped coil was connected to a high frequency (30–80 kHz) electric power supply (LT-51, Lantech Co, Taiwan) which could adjust the power output from 1.5 kW to 15 kW. The power will be changed to control the raising rate of temperature in the study.

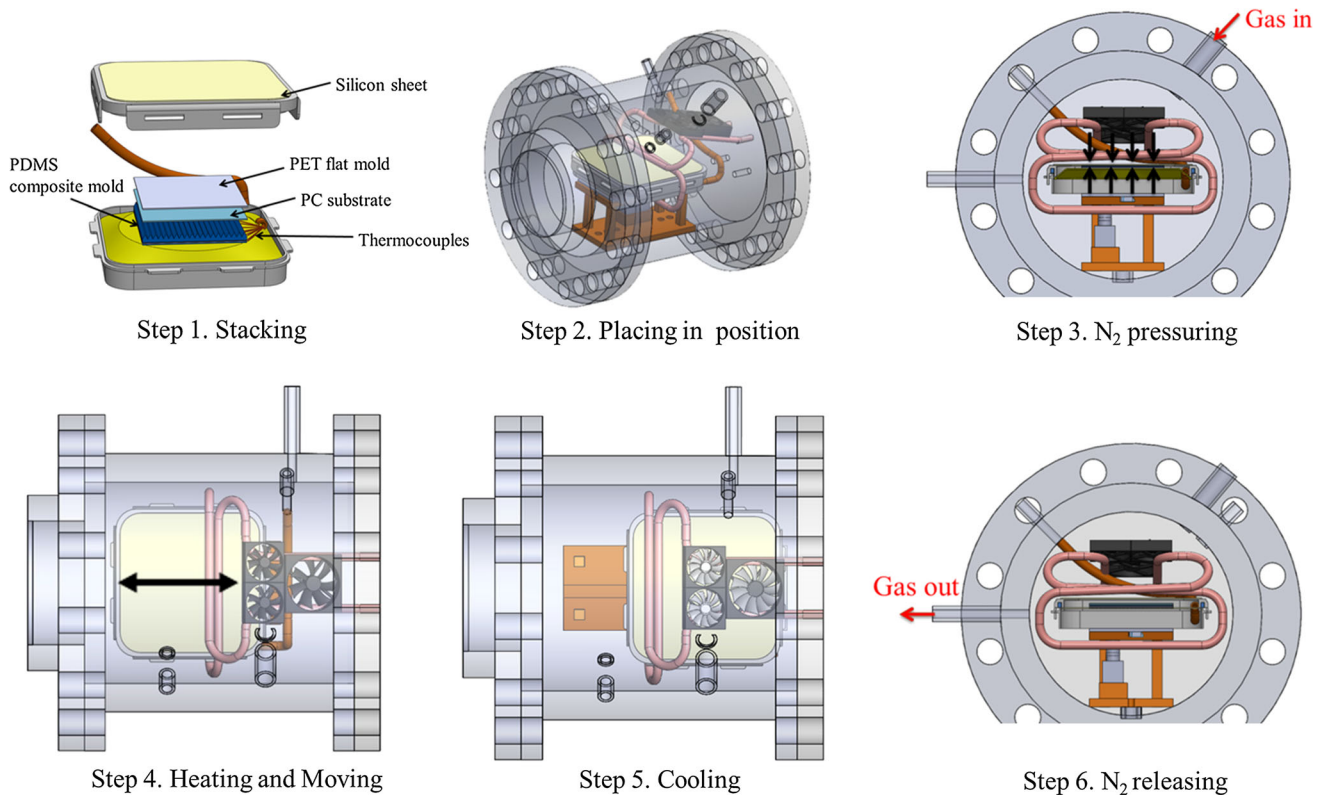


Fig. 11 Hot embossing procedure

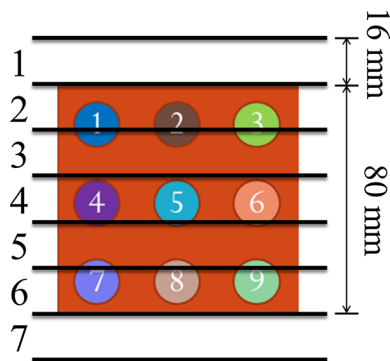


Fig. 12 Position of moving station 1–7

Table 1 Moving condition

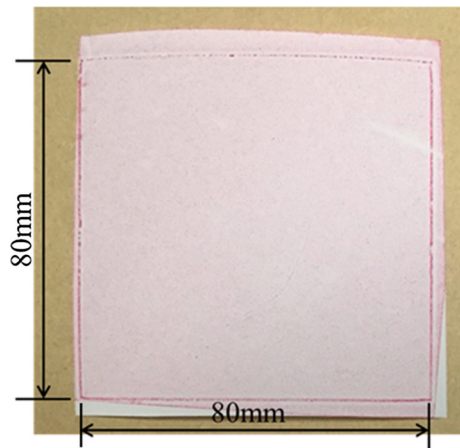
Station	State
1	20 s
1–4	24 mm/s
4	1 s
4–6	32 mm/s
6	12 s
7	0 s

Table 2 Schematic of a single-factor experiment for hot embossing

No. exp	Mold temp (°C)	Molding pressure (kgf/cm <sup>2</sup> )
1	170	5
2	180	5
3	190	5
4	200	5
5	210	5
6	200	1
7	200	2
8	200	3
9	200	4
10	200	7.5
11	200	10

### 3.5 Procedure

Figure 11 showed the moving induction heating hot embossing procedure, which progress were shown as follows: (1) The PET, substrate and mold were stacked up layer by layer. The polycarbonate substrate was the replicated material in the study. PDMS composite mold was with the microstructure on the PDMS layer, which was cast from nickel mold. The steel platen was the heating source which generated heat by the alternative magnetic field; (2)



**Fig. 13** Pressure distribution as displayed in the pre-scale film under the pressure of 1.0 Mpa

**Table 3** Heating rate (°C/s) in each station and points

Station	Points								
	1	2	3	4	5	6	7	8	9
1	4.6	4.4	5.3	1.6	1.7	1.8	0.2	0.2	0.2
2	6.9	7.1	7.5	4.6	4.9	4.9	1.1	1.1	1.2
3	7.4	8.4	8.6	11.1	10.1	10.8	3.4	3.5	3.6
4	6.2	6.2	6.4	15.5	13.6	15.9	5.3	5.2	5.7
5	2	2.5	2.3	10.2	10	11.7	9.8	8.7	9.7
6	1.2	1.7	1.3	4.1	3.2	4.1	8.2	7.7	8.1
7	0.5	0.6	0.5	0.7	0.9	1.2	3.3	3.6	3.5

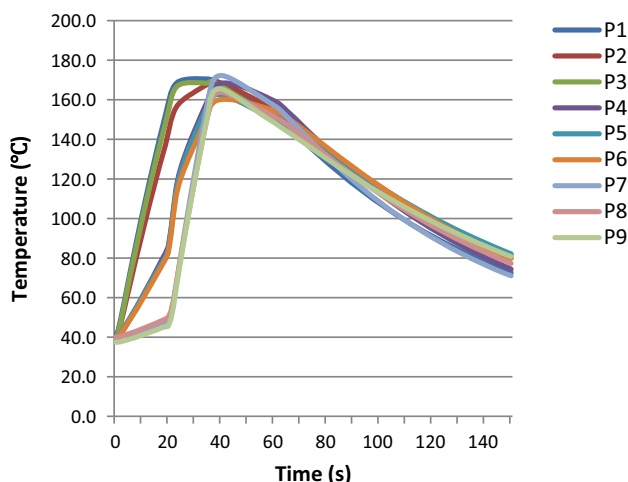


**Fig. 14** Measured temperature variation for moving induction heating

The mold was moving to the specific position; (3) The air filled into the chamber and the gas in the sealed box was forced out by the gas pressure in the chamber; (4) While the air pressure reached to embossing pressure ( $5\text{--}10\text{ kgf/cm}^2$ ), induction heating and moving device were turn on until

temperature reached to the molding temperature ( $170\text{--}210\text{ }^\circ\text{C}$  in the study); (5) After the temperature was reached, turn off the heating and moving power and turn on the cooling module until demolding temperature  $80\text{ }^\circ\text{C}$ ; (6) releasing the gas from the chamber and demolding the substrate from the PDMS composite mold.

The moving path was divided into 7 stations, each station was width of 16 mm as shown in Fig. 12. The moving setting used in the study was shown in Table 1. The coil heating at the station 1 last for the 20 s and the started mold moving by the speed of 24 mm/s and stop at station 4 and staying for 1 s. The mold started moving by the speed of 32 mm/s to the station 6, and staying at station 6 for 12 s. The induction heating in the moving process kept heating.

In most hot embossing studies, forming temperature and pressure were the important parameters to replication. In this study, single-factor experiment was applied to hot embossing including embossing temperature ( $170\text{--}210\text{ }^\circ\text{C}$ ) and molding pressure ( $5\text{--}10\text{ kg/cm}^2$ ). The parameters were shown in Table 2.

## 4 Results and discussion

### 4.1 Verification of pressure uniformity and performance of the coil

The pre-scale film (LLW-type,  $0.5\text{--}2.5\text{ Mpa}$ , Fuji, Japan) was employed to verify the uniformity of the imprinting pressure in this study. Figure 13 showed the pressure distribution under the condition of 1.0 MPa of gas pressure. It indicated that the pressure distribution of  $80 \times 80\text{ mm}^2$  area was uniform.

### 4.2 Heating rate

Table 3 showed the heating rate in each station and points. The highest heating rate appeared in middle station. On the contrary, top and bottom station showed the lowest heating rate when induction heating coil was staying above them. This phenomenon was verified on the end effect (Totten et al. 2004). To solve this situation, it can be modified by setting longer heating time at both ends of the mold.

Figure 14 showed the temperature variation during moving induction heating by the moving setting of Fig. 12b. The nine-point temperature measurement on the mold were heated up when the mold passed through the coil, and each point was heated up to  $170 \pm 10\text{ }^\circ\text{C}$  and total heating process took 36 s.

The strategy of adjusting the final temperature is by changing the power of induction heating device. Table 4 showed the power setting of molding temperature  $170\text{--}210\text{ }^\circ\text{C}$ . It showed the average temperature and

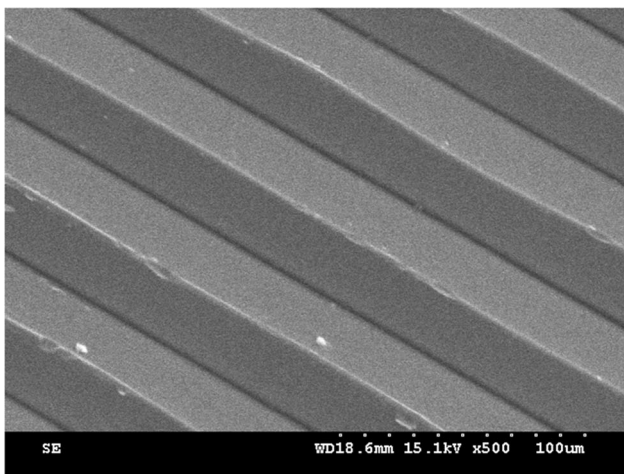


**Table 4** Power setting and temperature uniformity of different temperature

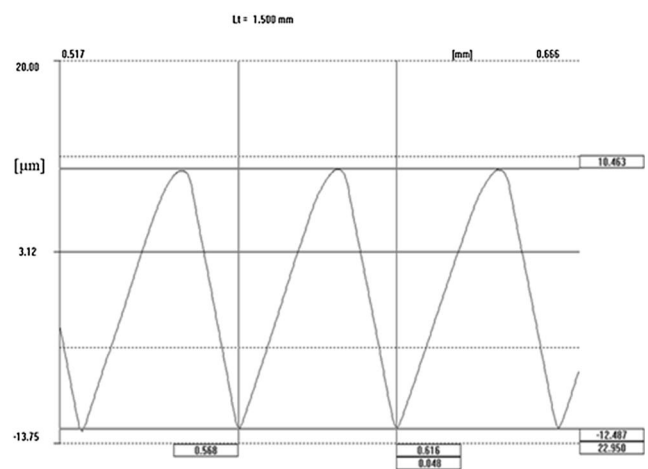
Molding temp. (°C)	Power (kW)	Temperature (°C)										
		P1	P2	P3	P4	P5	P6	P7	P8	P9	Avg	Range
170	3.15	170.7	169.1	169.3	168.5	162.7	160.3	172.3	163.8	165.6	166.9	12
180	3.45	177.7	175.6	174.0	183.0	179.2	174.5	189.3	180.5	186.2	180.0	15.3
190	4.05	197.5	192.6	191.8	194.2	188.3	184.4	197.1	189.4	194.6	192.2	13.1
200	4.35	204.6	199.3	197.6	211.7	204.0	198.4	203.5	193.7	200.8	201.5	18
210	4.5	210.3	206.1	204.5	220.0	211.9	207.2	224.1	212.6	220.2	213.0	19.6

**Table 5** Hot embossing experiment with various molding temperatures

Temp (°C)	Point										
	1	2	3	4	5	6	7	8	9	Avg (%)	Range (%)
170	34.1	31.4	33.7	23.4	20.4	22.1	39.6	36.3	28.3	29.9	19.2
180	47.7	45.0	40.4	75.2	65.1	48.0	97.5	95.5	98.5	68.1	58.1
190	96.6	96.4	97.9	94.8	89.8	94.9	97.0	97.8	98.2	95.9	8.4
200	98.2	97.6	97.1	95.3	96.2	98.3	96.4	96.3	97.1	96.9	3.0
210	96.1	96.5	97.9	96.1	94.7	95.9	96.6	97.1	97.2	96.5	3.1



(a)



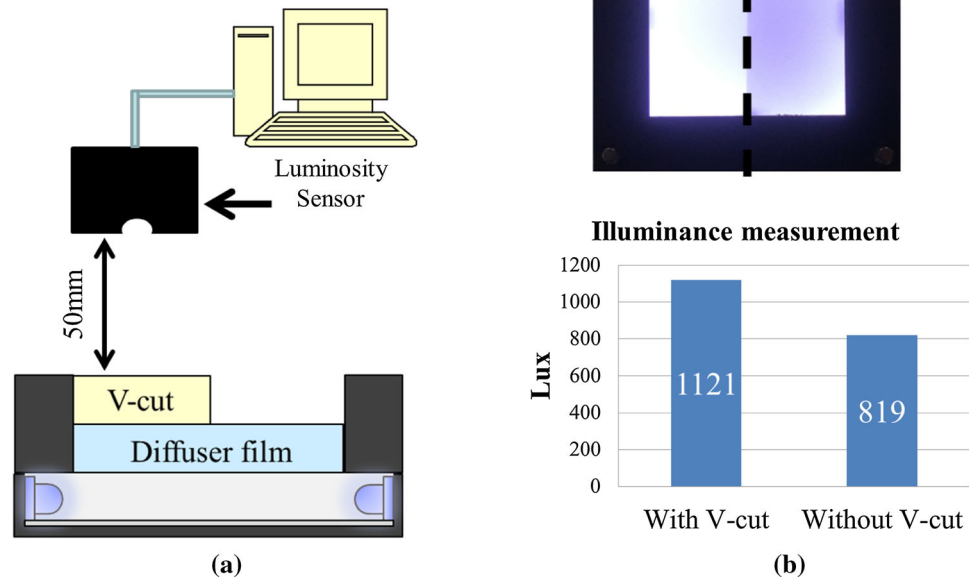
(b)

**Fig. 15** a SEM image and b surface profiles of the V-cut on the PC substrate

**Table 6** Hot embossing experiment with various molding pressures (molding temperature: 200 °C)

kgf/cm <sup>2</sup>	Point										
	1	2	3	4	5	6	7	8	9	Avg (%)	Range (%)
1	97.3	85.2	89.4	99.1	77.9	83	96.6	93.6	97.9	91.1	21.2
2	93.6	83.8	96.6	97.9	95.7	98.3	94.9	95.7	97	94.8	14.5
3	96.2	92.3	96.2	96.6	92.3	97.4	97.4	96.6	95.3	95.6	5.1
4	97	97	96.6	96.6	95.3	97	97.9	97	97	96.8	2.6
5	98.2	97.6	97.1	95.3	96.2	98.3	96.4	96.3	97.1	96.9	3
7.5	97.4	97	98.3	97.4	97	97.4	97.4	96.2	99.1	97.5	3
10	96.2	97.4	97.9	94.9	97.4	94.5	96.6	97.4	98.7	96.8	4.3

**Fig. 16** **a** Schematic diagram of illuminance measurement. **b** The image of the LED light passed through V-cut film and without V-cut film and the Illuminance measurement result



temperature difference from nine-point measurement. The temperature difference was under 20 °C in each molding temperature from 170 to 210 °C.

### 4.3 Replication rates of V-cut on PC substrate

In this study, the factor of temperature (170–210 °C) and pressure (5–10 kg/cm<sup>2</sup>) were used in the study and discussed the effect of the replication rate, as shown in Table 2. The replication of sample is expressed as follows:

$$\text{Replication (\%)} = \frac{\text{height of the microstructure in the embossed substrate}}{\text{height of the microstructure in the mold}} \times 100\% \quad (2)$$

In the impact of the temperature on the hot embossing, it showed the replication rate of nine-point measured corresponding to the molding temperature from 170 to 210 °C at a molding pressure of 5 kgf/cm<sup>2</sup> in Table 5. The average replication rates to molding temperature 170 °C, 180 °C and 190 °C were 29.9%, 68.1%, and 95%, respectively. It showed that the molding temperature obviously effected on the replication rate. When molding temperature at 200 °C and 210°, the average replication rates were 96.9% and 96.5%. It shows that molding temperature of 200 °C could achieved the best replication rate 96.9% of PC in the moving induction heating process. The SEM image and surface profiles of the V-cut replicated by molding temperature 200 °C and pressure 5 kgf/cm<sup>2</sup> are shown in Fig. 15.

In the effect of the pressure on the hot embossing, the nine-point measured of replication rate with molding pressure 1–10 kgf/cm<sup>2</sup> at molding temperature 200 °C was shown in Table 6. The average replication rates is reached 91.1% at the molding pressure 1 kgf/cm<sup>2</sup> and reach 96.8% at the molding pressure 4 kgf/cm<sup>2</sup>. The results showed the average replication rate didn't increase obviously with pressure increasing 4–10 kgf/cm<sup>2</sup>. According to the results of increasing temperature and pressure, the temperature showed more effective in replication rate.

### 4.4 Optical properties of the replicated V-cut

In many commercial products, V-cut structures have been widely used as the brightness enhancement film. To verify and inspect the optical properties of the replicated V-cut on PC sheet, the Luminosity Sensor (TSL2561, TAOS Inc., USA) was employed to measure the illuminance as shown in Fig. 16a. The results showed the V-cut film could enhance 36.8% illuminance comparing to without V-cut film, as shown in (b). Obviously, film with v-cut displayed better brightness than film without V-cut. The results demonstrated that the replicated V-cut film can be used as enhancement film.

## 5 Conclusion

This study successfully extended the embossing area with single turn coil, moving mechanism and uniform pressure by gas, having the rapid heating, uniform pressure and

extended ability of embossing area. In addition, the PDMS composite mold with microstructure solved the problem of microstructure effect in metal mold via induction heating. Based on simulation and experiment results, the following conclusions are obtained.

- The hot embossing area of  $80 \times 80 \text{ mm}^2$  has successfully replicate 96% of micro V-cut. It demonstrated the moving induction heating with gas-assisted hot embossing process provided the new way to increase the embossing area without longer coil or high power induction heating device.
- In the mold moving, the middle area showed highest heating rate ( $\sim 13 \text{ }^\circ\text{C/s}$ ) and the both end showed the lowest heating rate ( $\sim 5 \text{ }^\circ\text{C/s}$ ). The different heating rate of the mold can be compensating by adjusting the coil staying time in each area. The embossing temperature could be adjusting by increasing the power of induction heating device without change the moving path and each temperature difference was under  $20 \text{ }^\circ\text{C}$ .
- The temperature showed the greater effect of replication rate than the pressure.
- The replicated V-cut film can increase the front illuminance by 36%.

## References

- Chen Q, Zhang L, Chen G (2014) Far infrared-assisted embossing and bonding of poly(methyl methacrylate) microfluidic chips. *RSC Adv* 4(99):56440–56444
- Gao H, Tan H, Zhang W, Morton K, Chou SY (2006) Air cushion press for excellent uniformity, high yield, and fast nanoimprint across a 100 mm field. *Nano Lett* 6(11):2438–2441
- Goral VN, Hsieh Y-C, Petzold ON, Faris RA, Yuen PK (2011) Hot embossing of plastic microfluidic devices using poly(dimethylsiloxane) molds. *J Micromech Microeng* 21(1):017002
- Hocheng H, Wen TT (2008) Innovative approach to uniform imprint of micron and submicron features. *J Achiev Mater Manuf Eng* 28(1):79–82
- Hong S-K, Heo Y-M, Kang J (2008) Replication of polymeric micro patterns by rapid thermal pressing with induction heating apparatus. In: 2008 3rd IEEE international conference on nano/micro engineered and molecular systems, pp 911–915
- Lin H-L, Chen S-C, Jeng M-C, Minh PS, Chang J-A, Hwang J-R (2012) Induction heating with the ring effect for injection molding plates. *Int Commun Heat Mass Transf* 39(4):514–522
- Nian S-C, Tsai T-H, Huang M-S (2016) Novel inductive hot embossing for increasing micromolding efficiency. *Int Commun Heat Mass Transf* 70:38–46
- Seunarine K, Gadegaard N, Riehle MO, Wilkinson CDW (2006) Optical heating for short hot embossing cycle times. *Microelectron Eng* 83(4–9):859–863
- Sun Y, Wang Y, Yang X, Pang L (2013) A novel coil distribution for transverse flux induction heating. *Phys Proc* 50:32–37
- Totten GE, Funatani K, Xie L (2004) Handbook of metallurgical process design. CRC Press, Boca Raton
- Xie P et al (2014) Rapid hot embossing of polymer microstructures using carbide-bonded graphene coating on silicon stampers. *Surf Coat Technol* 258:174–180
- Yang H-A, Lin C-W, Peng C-Y, Fang W (2006) On the selective magnetic induction heating of micron scale structures. *J Micromech Microeng* 16(7):1314
- Zhang B, Cui J, Duan J, Cui M (2017) A new fabrication method for nano-gratings based on the high flexibility of PDMS. *Opt Laser Technol* 92:206–210

**Publisher's Note** Springer Nature remains neutral with regard to jurisdictional claims in published maps and institutional affiliations.